The impact of the non-perturbative parameters in the PB method on the predictions for low energy DY measurements

REF 2019

• Ola Lelek [1] Francesco Hautmann [1,2] Hannes Jung [1,3]
Mees van Kampen [1] Lissa Keersmaekers [1] Mikel Mendizabal Morentin [4]

[1]University of Antwerp (UAntwerp)

[2]University of Oxford

[3]Deutsches Elektronen-Synchrotron (DESY)

[4]Euskal Herriko Unibertsitatea

Introduction

The PB method :

- valid in a wide range of x, $k_\perp$, μ^2
- applicable to exclusive observables & MC generators
- connection to DGLAP

PB method is successfully applied to the DY at the LHC see talk of Qun Wang

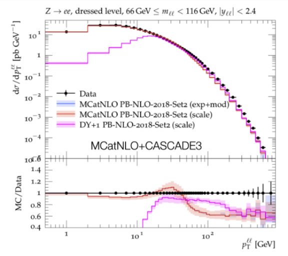

Phys. Rev. D100, 074027 (2019). 1906.00919

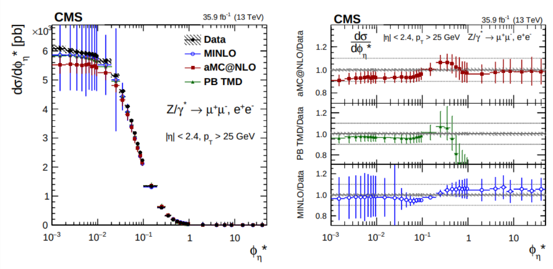

CMS, A. M. Sirunyan et al. (2019). 1909.04133

This talk:

1. examine in detail non-perturbative parameters in PB method
2. assess their impact on
   - TMDs
   - DY at the LHC
   - DY at low energies

Non-perturbative parameters in PB evolution equations

The PB evolution equation:

JHEP 1801 (2018) 070

$$\widetilde{A}_a\left(x, \boldsymbol{k}, \mu^2\right) = \Delta_a\left(\mu^2, \mu_0^2\right) \widetilde{A}_a\left(x, \boldsymbol{k}, \mu_0^2\right) + \sum_b \int \frac{\mathrm{d}^2 \boldsymbol{\mu}'}{\pi \mu'^2} \Theta\left(\mu^2 - \mu'^2\right) \Theta\left(\mu'^2 - \mu_0^2\right)$$

$$\times \quad \int_x^{z_M} \mathrm{d}z \, \frac{\Delta_a\left(\mu^2, \mu_0^2\right)}{\Delta_a\left(\mu'^2, \mu_0^2\right)} \, P_{ab}^R\left(z, \alpha_s((1-z)^2 \mu'^2)\right) \widetilde{A}_b\left(\frac{x}{z}, \boldsymbol{k} + (1-z)\boldsymbol{\mu}', \mu'^2\right)$$

Where do the non-perturbative parameters enter?

Non-perturbative parameters in PB evolution equations

The PB evolution equation:

JHEP 1801 (2018) 070

$$\widetilde{A}_a\left(x, \boldsymbol{k}, \mu^2\right) = \Delta_a\left(\mu^2, \mu_0^2\right) \widetilde{A}_a\left(x, \boldsymbol{k}, \mu_0^2\right) + \sum_b \int \frac{\mathrm{d}^2 \boldsymbol{\mu}'}{\pi \mu'^2} \Theta\left(\mu^2 - \mu'^2\right) \Theta\left(\mu'^2 - \mu_0^2\right)$$

$$\times \quad \int_x^{z_M} \mathrm{d}z \, \frac{\Delta_a\left(\mu^2, \mu_0^2\right)}{\Delta_a\left(\mu'^2, \mu_0^2\right)} \, P_{ab}^R\left(z, \alpha_s((1-z)^2 \mu'^2)\right) \widetilde{A}_b\left(\frac{x}{z}, \boldsymbol{k} + (1-z)\boldsymbol{\mu}', \mu'^2\right)$$

Where do the non-perturbative parameters enter?

- Initial distribution: $\widetilde{A}_{0,a}(x, \boldsymbol{k}_0, \mu_0) = \widetilde{f}_{0,a}(x, \mu_0) \cdot \exp(-\boldsymbol{k}_0{}^2/\sigma^2)$
  where $\sigma^2 = q_s^2/2$
- soft gluon resolution scale: $z_M = 1 - \frac{q_0}{\mu'}$ arXiv:1908.08524 & talk of Mees van Kampen
  marked in equation above, but also in the Sudakov form factor:

$$\Delta_a(\mu^2, \mu_0^2) = \exp\left(-\sum_b \int_{\mu_0^2}^{\mu^2} \frac{\mathrm{d}\mu'^2}{\mu'^2} \int_0^{z_M} \mathrm{d}z \; z \; P_{ba}^R\left(z, \alpha_s\left((1-z)^2 \mu'^2\right)\right)\right)$$

---

notation: $k = (k^0, k^1, k^2, k^3) = (E_k, \boldsymbol{k}, k^3)$, where $\boldsymbol{k} = (k^1, k^2)$, and $k_\perp = |\boldsymbol{k}|$, $\mu' = \sqrt{\boldsymbol{\mu}'^2}$

Non-perturbative parameters in PB evolution equations

The PB evolution equation:

JHEP 1801 (2018) 070

$$\widetilde{A}_a\left(x,\boldsymbol{k},\mu^2\right)=\Delta_a\left(\mu^2,\mu_0^2\right)\widetilde{A}_a\left(x,\boldsymbol{k},\mu_0^2\right)+\sum_b\int\frac{\mathrm{d}^2\boldsymbol{\mu}'}{\pi\mu'^2}\Theta\left(\mu^2-\mu'^2\right)\Theta\left(\mu'^2-\mu_0^2\right)$$
$$\times\quad\int_x^{z_M}\mathrm{d}z\,\frac{\Delta_a\left(\mu^2,\mu_0^2\right)}{\Delta_a\left(\mu'^2,\mu_0^2\right)}\,P_{ab}^R\left(z,\alpha_s((1-z)^2\mu'^2)\right)\widetilde{A}_b\left(\frac{x}{z},\boldsymbol{k}+(1-z)\boldsymbol{\mu}',\mu'^2\right)$$

Where do the non-perturbative parameters enter?

- Initial distribution: $\widetilde{A}_{0,a}(x,\boldsymbol{k}_0,\mu_0)=\widetilde{f}_{0,a}(x,\mu_0)\cdot\exp(-{\boldsymbol{k}_0}^2/\sigma^2)$
  where $\sigma^2=q_s^2/2$
- soft gluon resolution scale: $z_M=1-\frac{q_0}{\mu'}$ arXiv:1908.08524 & talk of Mees van Kampen
  marked in equation above, but also in the Sudakov form factor:

$$\Delta_a(\mu^2,\mu_0^2)=\exp\left(-\sum_b\int_{\mu_0^2}^{\mu^2}\frac{\mathrm{d}\mu'^2}{\mu'^2}\int_0^{z_M}\mathrm{d}z\;z\;P_{ba}^R\left(z,\alpha_s\left((1-z)^2\mu'^2\right)\right)\right)$$

notation: $k=(k^0,k^1,k^2,k^3)=(E_k,\boldsymbol{k},k^3)$, where $\boldsymbol{k}=(k^1,k^2)$, and $k_\perp=|\boldsymbol{k}|$, $\mu'=\sqrt{\boldsymbol{\mu}'^2}$

Impact of soft gluon resolution scale on TMDs

$$\Delta_a(\mu^2, \mu_0^2) = \exp\left(- \sum_b \int_{\mu_0^2}^{\mu^2} \frac{\mathrm{d}\mu'^2}{\mu'^2} \int_0^{z_M} \mathrm{d}z \; z \; P_{ba}^R \left(z, \alpha_s\left((1-z)^2 \mu'^2\right)\right)\right)$$

$z_M = 1 - q_0/\mu'$

Sudakov: probability of an evolution without any resolvable branching bewteen μ_0 and μ

bigger z_M (= smaller q_0) $\rightarrow$ smaller Sudakov $\rightarrow$ more branchings

- with low q_0 intrinsic $k_\perp$ distribution smeared by the evolution
  more branchings which fill matching region of intrinsic $k_\perp$ and evolution ($q_\perp^2 = (1-z)^2 \mu'^2$)
- large q_0: matching of intrinsic distribution with the evolution visible
- lower $q_0 \longleftrightarrow$ lower TMD in the low $k_\perp$ and higher in the high $k_\perp$ region
- NB: gluons at low x: $1/z$ term in P^R smears the contribution from intrinsic $k_\perp$, low q_0 dominates the whole spectrum

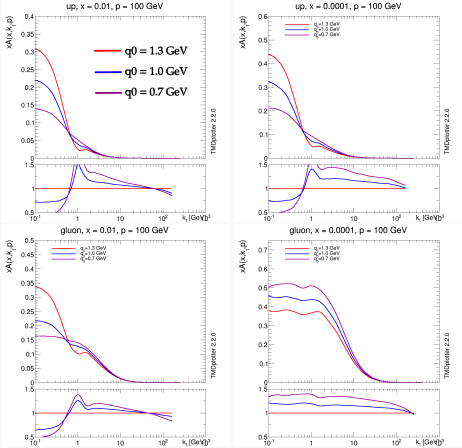

Impact of intrinsic $k_\perp$ on TMDs

$\widetilde{A}_{0,a}(x, k_{\perp 0}, \mu_0) = \widetilde{f}_{0,a}(x, \mu_0) \cdot \exp(-k_{\perp 0}^2/\sigma^2)$
where $\sigma^2 = q_s^2/2$

- q_s affects only the low $k_\perp$ region
- with smaller q_s values, TMDs at low $k_\perp$ larger
- with large q_s smooth matching of intrinsic $k_\perp$ and evolution
- NB: gluon at small x: spectrum dominated by the evolution, the effect of q_s much less visible

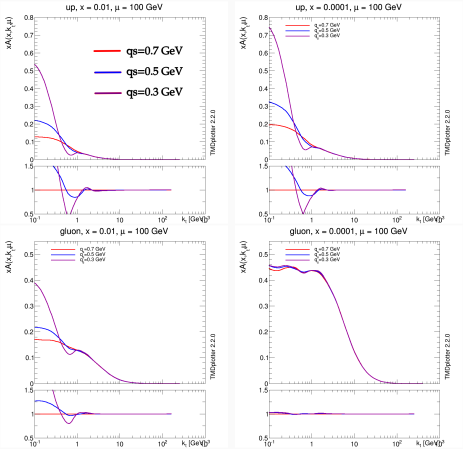

Application of the TMDs to measurements

Procedure: Phys. Rev. D99, 074008 (2019). 1804.11152

- DY collinear ME
- Generate $k_\perp$ of $q\overline{q}$ according to TMDs (m_{DY} fixed, x_1, x_2 change)
- compare with the measurement

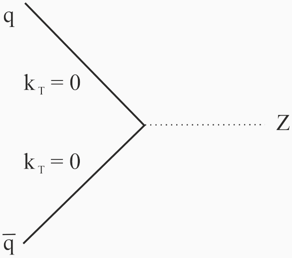

Application of the TMDs to measurements

Procedure: Phys. Rev. D99, 074008 (2019). 1804.11152

- DY collinear ME
- Generate $k_\perp$ of $q\bar{q}$ according to TMDs ($m_{\rm DY}$ fixed, x_1, x_2 change)
- compare with the measurement

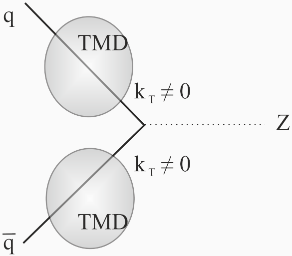

Impact of soft gluon resolution scale and intrinsic $k_\perp$ on DY spectrum at the LHC

Data: ATLAS 8 TeV measurement Eur. Phys. J. C76, 291 (2016)

Effect of q_0

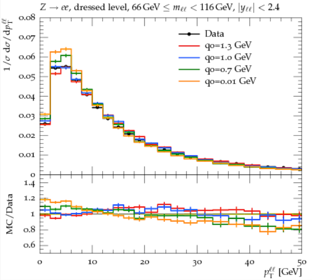

Strong dependence on q_0 observed, low $p_\perp$ region described better with $q_0 \approx 1$ GeV.

Effect of q_s

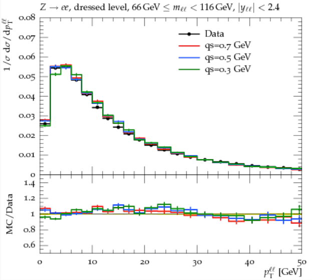

Very slight effects of q_s only visible in the very low $p_\perp$ region

What about low energy DY?

We apply the PB method to the NUSEA (E866) data

fix target experiment at Fermilab for proton-hydrogen and proton-deuterium collisions at $\sqrt{s} = 38.8$ GeV

Phys. Rev. Lett. 80, 3715 (1998), J. C. Webb, Ph.D. Thesis, hep-ex/0301031, 2003.

Toy Model: TMDs with no fit, LO ME

Impact of soft gluon resolution scale and intrinsic $k_\perp$ on DY spectrum at the LHC

Data: ATLAS 8 TeV measurement Eur. Phys. J. C76, 291 (2016)

Effect of q_0

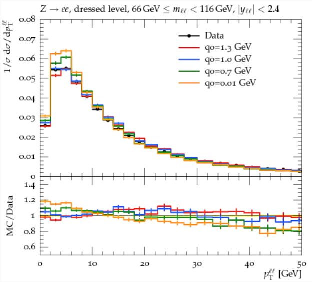

Strong dependence on q_0 observed, low $p_\perp$ region described better with $q_0 \approx 1$ GeV.

Effect of q_s

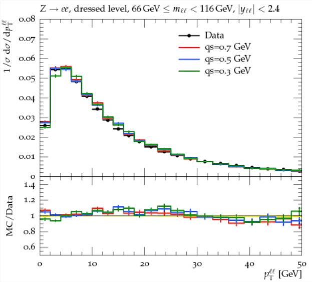

Very slight effects of q_s only visible in the very low $p_\perp$ region

What about low energy DY?

We apply the PB method to the NUSEA (E866) data

fix target experiment at Fermilab for proton-hydrogen and proton-deuterium collisions at $\sqrt{s} = 38.8$ GeV

Phys. Rev. Lett. 80, 3715 (1998), J. C. Webb, Ph.D. Thesis, hep-ex/0301031, 2003.

Toy Model: TMDs with no fit, LO ME

Dynamic z_M

q_0 dependence

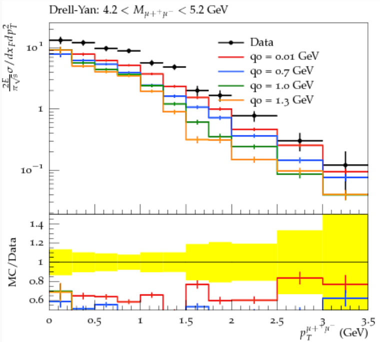

Here: $q_s = 0.5$ GeV

Strong dependence on q_0

q_s dependence

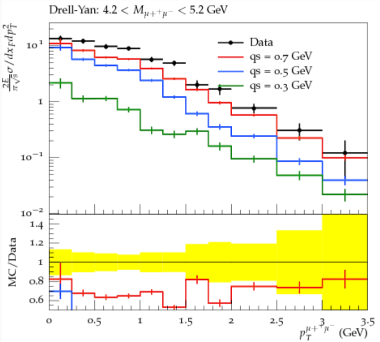

Here: $q_0 = 1.0$ GeV

Strong dependence on q_s

Prediction with $q_s = 0.3$ GeV much lower → matching between intrinsic $k_\perp$ distribution and evolution

---

Toy Model: No fit for TMDs, LO ME with K-factor = 1.8 hep-ex/0301031

Dynamic z_M

q_0 dependence

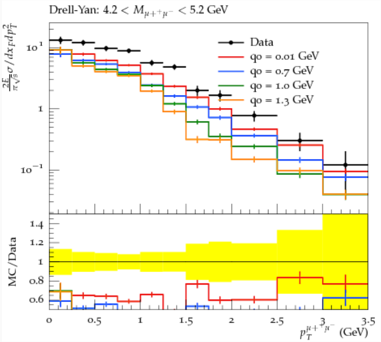

Here: $q_s = 0.5$ GeV

Strong dependence on q_0

q_s dependence

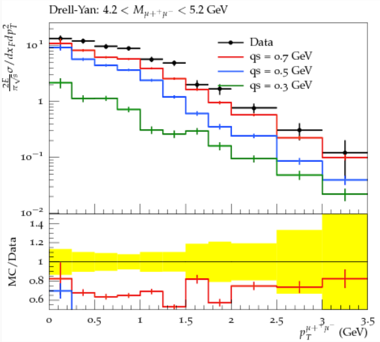

Here: $q_0 = 1.0$ GeV

Strong dependence on q_s

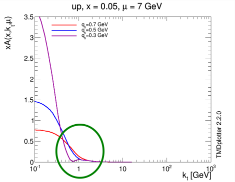

Prediction with $q_s = 0.3$ GeV much lower $\rightarrow$ matching of intrinsic $k_\perp$ distribution and evolution

---

Toy Model: No fit for TMDs, LO ME with K-factor = 1.8 hep-ex/0301031

Dynamic z_M

q_0 dependence

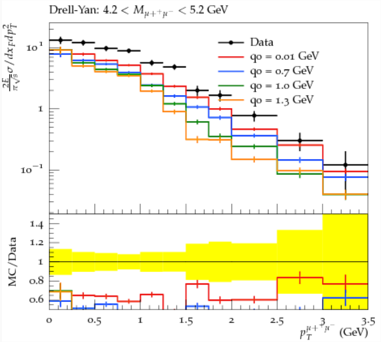

Here: $q_s = 0.5$ GeV

Strong dependence on q_0

q_s dependence

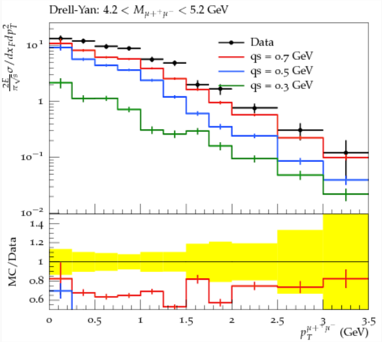

Here: $q_0 = 1.0$ GeV

Strong dependence on q_s

Data described similarly well by TMDs with different combinations of q_0 and q_s
$\rightarrow$ q_0 and q_s are not independent
One needs to use different datasets since they give complementary information (NUSEA, ATLAS,...)

Toy Model: No fit for TMDs, LO ME with K-factor = 1.8 hep-ex/0301031

NUSEA with Benchmark PB TMDs and MCatNLO method

Results with PBSet2 obtained from the fit with the MCatNLO subtraction

PhysRevD.99.074008 & talk of Sara Taheri Monfared

Procedure for PB TMDs and MCatNLO: Phys. Rev. D100, 074027 (2019) & talk of Qun Wang

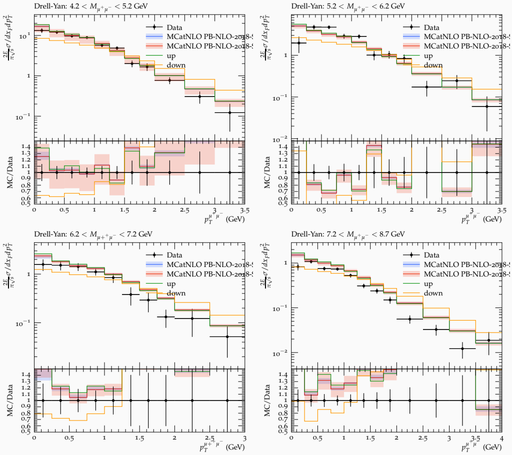

Band from the fit: experimental + model (blue), scale variation (orange)

Variation of q_s not included in the fit, shown separately (variations by factor of 2)

Very good description of the low energy and low mass DY with PB TMDs and MCatNLO

PB method applicable in a wide kinematic range

PB TMDs and MCatNLO subtraction scheme

PB TMDs with MCatNLO subtraction method: Phys. Rev. D100, 074027 (2019)

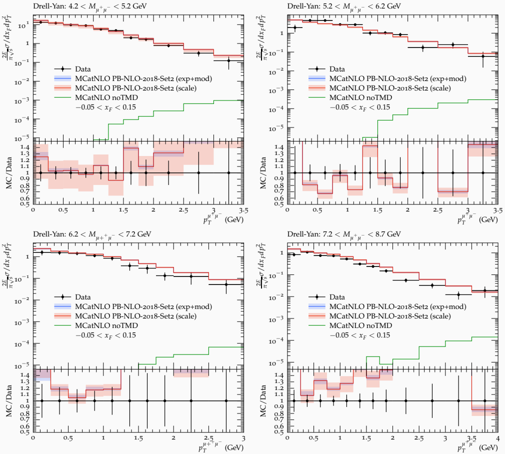

MCatNLO prediction (ME after the subtraction, not physical) orders of magnitude smaller than data. The phase space is then populated with TMDs

Transition between the low and high $p_\perp$ physics treated by the MCatNLO method

Outlook: application the PHENIX

VERY FRESH RESULT! ☺

pp collisions at $\sqrt{s} = 200~\mathrm{GeV}$ at the RHIC Data: PhysRevD.99.072003

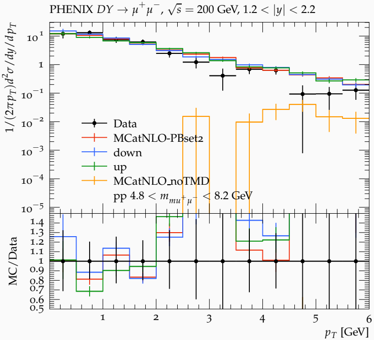

Very good description of the low energy and low mass DY with PB TMDs and MCatNLO again!

PB method applicable in a wide kinematic range

Summary & Conclusions

- The effect of intrinsic $k_\perp$ distribution and soft gluon resolution scale studied in TMDs, DY at LHC and DY at low energies
- NUSEA & PHENIX data described by the benchmark PB TMDs with MCatNLO method
  PB method applicable in a wide kinematic range
- sensitivity of the NUSEA data to the intrinsic $k_\perp$ and soft gluon resolution scale illustrated
- Presented results important for the further development of the fit procedure within the PB method

Summary & Conclusions

- The effect of intrinsic $k_\perp$ distribution and soft gluon resolution scale studied in TMDs, DY at LHC and DY at low energies
- NUSEA & PHENIX data described by the benchmark PB TMDs with MCatNLO method
  PB method applicable in a wide kinematic range
- sensitivity of the NUSEA data to the intrinsic $k_\perp$ and soft gluon resolution scale illustrated
- Presented results important for the further development of the fit procedure within the PB method

Thank you!

backup

Impact of q_s on TMDs, $\mu = 10$ GeV

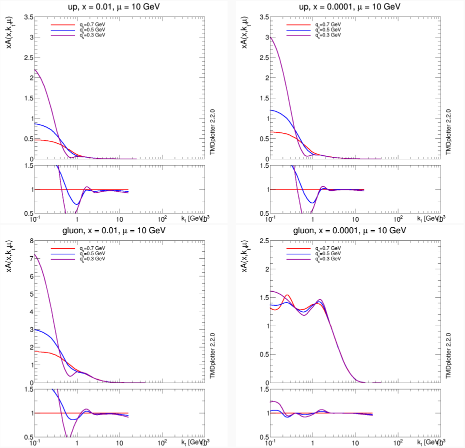

Impact of q_s on iTMDs

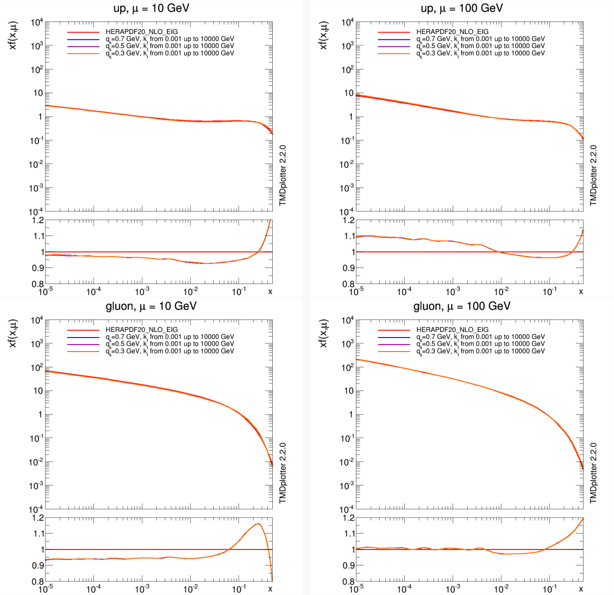

No difference between different q_s values (blue, violet, orange curves on top of each other.
HERAPDF2.0 used as a starting distribution for PB TMDs shown for comparison.

Impact of q_0 on TMDs, $\mu = 10\ \mathrm{GeV}$

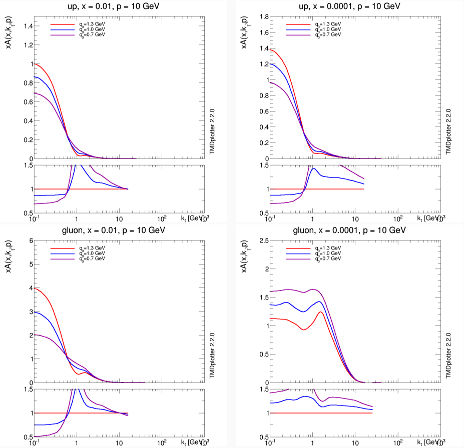

Z boson $p_\perp$, q_s dependence

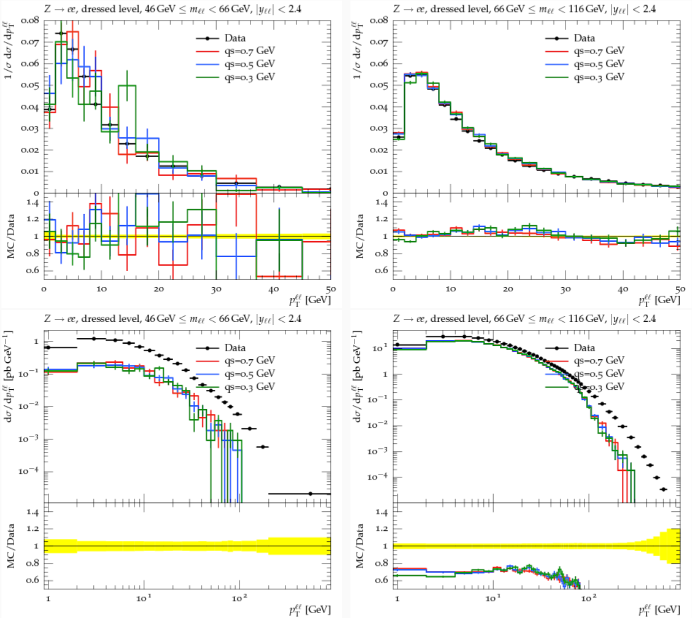

Z boson $p_\perp$, q_0 dependence

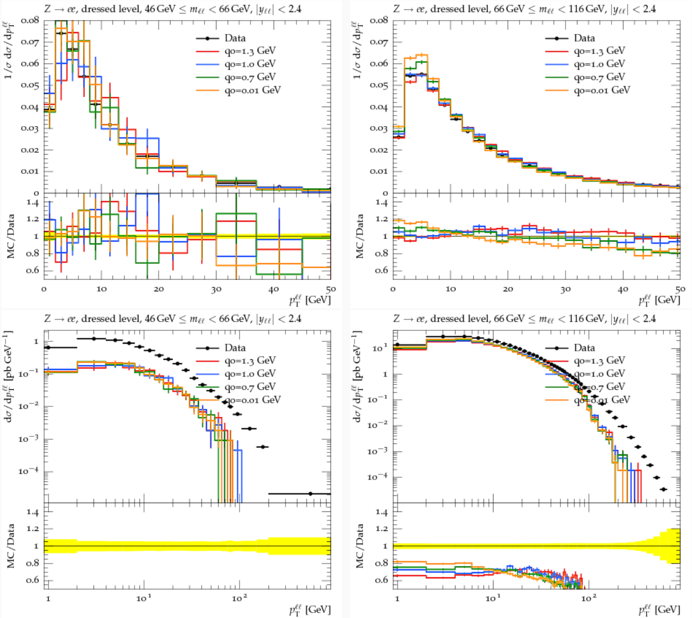

NUSEA, Dynamic z_M, other mass bins

q_0 dependence

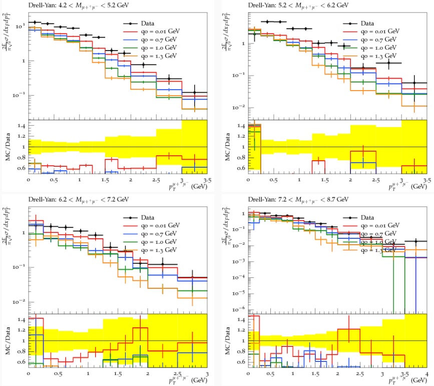

Here: $q_s = 0.5$ GeV

Strong dependence on q_0

q_s dependence

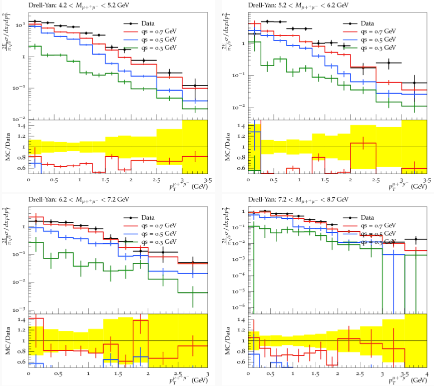

Here: $q_0 = 1.0$ GeV

Strong dependence on q_s

Toy Model: No fit for TMDs, LO ME with K-factor = 1.8 hep-ex/0301031